STEM CELLS AND DEVELOPMENT
Volume 22, Number 24, 2013

DOI: 10.1089/scd.2013.0064

Platelet Rich Plasma Clot Releasate Preconditioning Induced PI3K/AKT/NFκB Signaling Enhances Survival and Regenerative Function of Rat Bone Marrow Mesenchymal Stem Cells in Hostile Microenvironments

Yan Peng,[1–3,*] Sha Huang,[3,4,*] Yan Wu,[5] Biao Cheng,[1] Xiaohu Nie,[2] Hongwei Liu,[6] Kui Ma,[3] Jiping Zhou,[3] Dongyun Gao,[3] Changjiang Feng,[3] Siming Yang,[3] and Xiaobing Fu[3,4]

Mesenchymal stem cells (MSCs) have been optimal targets in the development of cell based therapies, but their limited availability and high death rate after transplantation remains a concern in clinical applications. This study describes novel effects of platelet rich clot releasate (PRCR) on rat bone marrow-derived MSCs (BM-MSCs), with the former driving a gene program, which can reduce apoptosis and promote the regenerative function of the latter in hostile microenvironments through enhancement of paracrine/autocrine factors. By using reverse transcription–polymerase chain reaction, immunofluorescence and western blot analyses, we showed that PRCR preconditioning could alleviate the apoptosis of BM-MSCs under stress conditions induced by hydrogen peroxide (H_2O_2) and serum deprivation by enhancing expression of vascular endothelial growth factor and platelet-derived growth factor (PDGF) via stimulation of the platelet-derived growth factor receptor (*PDGFR*)/*PI3K*/*AKT*/*NF-κB* signaling pathways. Furthermore, the effects of PRCR preconditioned GFP-BM-MSCs subcutaneously transplanted into rats 6 h after wound surgery were examined by histological and other tests from days 0–22 after transplantation. Engraftment of the PRCR preconditioned BM-MSCs not only significantly attenuated apoptosis and wound size but also improved epithelization and blood vessel regeneration of skin via regulation of the wound microenvironment. Thus, preconditioning with PRCR, which reprograms BM-MSCs to tolerate hostile microenvironments and enhance regenerative function by increasing levels of paracrine factors through *PDGFR-α*/*PI3K*/*AKT*/*NF-κB* signaling pathways would be a safe method for boosting the effectiveness of transplantation therapy in the clinic.

Introduction

During the last decade, widespread experimental studies in animal models and clinical settings have shown the safety, feasibility and efficacy of mesenchymal stem cells (MSCs) in therapies for various diseases. The promising results were not only attributed to their inherent characteristics of self-renewal, unlimited capacity for proliferation, ability to cross lineage restrictions, and adopt different phenotypes [1], but also to endocrine or paracrine factors produced by MSCs [2–8]. These cells have been the focus of both basic and clinical research in regenerative medicine. However, the large numbers of required cells and massive cell death in hostile environments have been impediments to successful MSC-based therapy [9]. For instance, transplanted bone marrow-derived mesenchymal stem/stromal cells (BM-MSCs) have been reported to often fail engraftment within the bone marrow (BM) partly due to the poor cell viability of donor cells. Additionally, the therapeutic effects of transplanted MSCs in myocardial infarction appear to be limited by the poor survival of donor cells in the injured myocardial tissue [10,11]. The underlying cause of the massive MSC death is multifactorial, and the prime factors responsible may be the loss of trophic factors, local tissue ischemia, production of

[1]The Key Laboratory of Trauma Treatment & Tissue Repair of Tropical Area, PLA, Department of Plastic Surgery, Guangzhou General Hospital of Guangzhou Command, Guangzhou, People's Republic of China.
[2]Southern Medical University, Guangzhou, People's Republic of China.
[3]Burns Institute, Trauma Center of Postgraduate Medical College, The First Affiliated Hospital, General Hospital of PLA, Beijing, People's Republic of China.
[4]Wound Healing and Cell Biology Laboratory, Institute of Basic Medical Sciences, General Hospital of PLA, Beijing, People's Republic of China.
[5]Heilongjiang Key Laboratory of Anti-Fibrosis Biotherapy, Mudanjiang Medical College, Mudanjiang, People's Republic of China.
[6]Key Laboratory for Regenerative Medicine, Ministry of Education, Department of Plastic Surgery, The First Affiliated Hospital of Jinan University, Guangzhou, People's Republic of China.
*These authors contributed equally to this work.

reactive oxygen species after ischemic reperfusion injury, and host inflammatory response mediators [12–14]. Considering that increasing the survival of stem cells may greatly enhance their effectiveness in transplantation therapy, several remedial approaches have been suggested, such as combining preconditioning (eg, ischemic/hypoxia preconditioning [15,16], pharmacological preconditioning [17], heat shock preconditioning [18,19], cytokine preconditioning [20,21]) and genetic modulation (eg, transgenes encoding for growth factors [22–24] or antiapoptotic factors [25–27]). However, these methods have not yielded significantly improved transplantation outcomes, and a more beneficial, simpler and safer approach is needed for future clinical applications.

Platelet rich plasma (PRP) has been used clinically in humans since the 1970s for its healing properties attributed to autologous growth factors and secretory proteins [28]. Recently, PRP was used for skin rejuvenation and inhibition of pre-adipocyte apoptosis in vitro [29,30]. It has also been shown to serve as a substitute for animal serum for the intended clinical application of stem cell therapy to eliminate the risk of xenogenic immune reactions, infections with bovine viruses and prions, as well as avoid high batch-to-batch variations [31]. It has further been indicated to enhance MSC proliferation, chemotaxis, fibroblastoid colony-forming unit (CFU-f) frequency and chondrogenic, adipogenitic or osteoblastic differentiation [32–34].

The mechanistic roles of PRP in both pathological situations and cell expansion have also been studied intensely. For instance, in relation to angiogenesis, Eppley et al. [35] reported that PRP can help stimulate endothelial cells near their application site and favor their proliferation and angiogenesis. Moreover, Hu et al. [36] concluded that PRP induces mRNA expression of vascular endothelial growth factor (VEGF) and platelet-derived growth factor (PDGF) in rat BM stromal cells, which potentially contributes to the initiation of angiogenesis and bone regeneration. However, the implications of MSC survival in a hostile environment and the exact cell regenerative or paracrine functions of MSCs with PRP intervention have not yet been fully clarified.

Based on the clinical need and rationale, we speculated that platelet rich clot releasate (PRCR) preconditioning can induce MSCs to promote self-protection in a hostile microenvironment. Therefore, we designed the present study to determine whether preconditioning with PRCR can exert antiapoptotic effects on BM-MSCs under stress conditions in vitro and ischemic/acute inflammatory conditions in vivo. We further determined whether the underlying mechanisms of the effects of PRCR preconditioning on BM-MSCs in hostile environments can be attributed to enhancement of paracrine factors through one specific or interrelated signaling ways, such as the well-known *AKT*, c-Jun N-terminal kinase (*JNK*), mitogen-activated protein kinase (*MAPK*) and *NF-κB* pathways. Finally, whether the survival or regenerative function of BM-MSCs can be enhanced by PRCR preconditioning after transplantation in acute skin wounds was investigated.

Materials and Methods

Ethics statement and animal care

All rats were housed and handled strictly in accordance with the recommendations of the Guide for the Care and Use of Laboratory Animals of the National Institutes of Health. The protocols were approved by the Committee on the Ethics of Animal Experiments of Burns Institute, the First Affiliated Hospital, General Hospital of PLA. All surgeries were performed using xylazine (20 mg/kg) and ketamine (100 mg/kg) as anesthesia, and all efforts were made to minimize suffering. We did not conduct research outside of our country of residence.

The blood for preparation of PRCR was obtained from six healthy male volunteers after receiving written consent and the approval of the ethics committee of Guangzhou General Hospital of Guangzhou Command, Guangdong, PLA.

Preparation of PRCR and measuring concentrations of growth factors

First, PRCR was prepared from blood of six healthy male volunteers (43–49 years old) who had not taken antiplatelet medications within 1 week of donation to explore the effects of PRCR concentration on the survival and regeneration of rat BM-MSCs. Furthermore, to minimize the possible influences of hormonal variation on the MSCs, we included only male and AB blood type donors. PRP was prepared via double centrifugation of blood as previously described [37]. In brief, 600 mL of whole blood (100 mL per person) was collected with acid citrate dextrose (ACD-A) tubes coated with an anticoagulating agent [10% (v/v); Sigma-Aldrich] and immediately centrifuged at 400 *g* for 10 min at 22°C to separate the platelet-containing plasma from the red cells (whole blood component separator; Terumo). The autologous packed red cells were infused back into each patient. The platelet-containing plasma was centrifuged at 5,000 *g* for an additional 5 min at 22°C to separate out platelet-poor plasma, and re-suspended platelet pellets were pooled for the PRP. The platelet number was then adjusted to $1{,}000 \times 10^9$/L. Finally, one part bovine thrombin stock solution (1,000 U/mL; Sigma-Aldrich) was added to nine parts PRP to activate the platelets. Each sample was incubated for 4 h at 37°C or overnight at 4°C. After the gel formation, the tubes were centrifuged at 12,000 *g* for 30 min at 4°C. The resulting supernatants from the clot preparation were collected as the PRCR, sterile filtered, and stored at −80°C until use. The concentrations of TGFß1, PDGF, and VEGF were evaluated by double-determinant immunoassays using commercially available kits (Quantikine R&D System, Inc. and Bender MedSystems, respectively) to validate the successful preparation of the PRCR. Analyses were conducted on 600 µL of the biological sample. The concentrations of TGFß1, PDGF and VEGF were 3,767 ng/mL (range 2,169–5,835 ng/mL; 95% CI 2,988–4,989 ng/mL), 5,773 pg/mL (range 1,896–11,032 pg/mL; 95% CI 3,742–8,502 pg/mL), and 922 pg/mL (range 343–1,294 pg/mL; 95% CI 667–1,358 pg/mL), respectively.

Isolation of BM-MSCs and cell culture

Primary rat BM-MSCs were obtained from male Sprague–Dawley rats (250–300 g, 6–10 weeks old) and isolated as previously described [38]. The collected cells were seeded at 2–$3 \times 10^3/\text{cm}^2$ in culture flasks filled with 12 mL of low-glucose Dulbecco's modified Eagle medium (DMEM; Gibco) supplemented with 10% fetal bovine serum (FBS; Gibco), 100 U/mL

penicillin, 100 μg/mL streptomycin and 2 m/mL-glutamine (Gibco) for incubation at 37°C in 5% CO_2. MSCs expanded at the 2rd–3th passage were identified and cultured for further experiments. Human aortic endothelial cells (HAECs) and rat GFP positive BM-MSCs obtained from a commercial source, (catalog number 304-05a; HAOEC; R492K-05, cryopreserved rat MSC; Cell Applications) were plated at 4,000 cells per cm^2, and cultured in endothelial growth medium (211–500; Cell Applications) or DMEM containing 10% FBS. These cells were trypsinized when reaching 70%–80% confluence and used at the 1st passage or 2nd–3rd passages.

Flow cytometry analysis and cellular phenotyping

The adherent cells at the 2rd–3rd passage were trypsinized, centrifuged, and then fixed in neutralized 2% paraformaldehyde solution for 30 min. The fixed cells were washed twice and re-suspended in PBS, incubated with fluorescein isothiocyanate (FITC)-labeled anti-rat CD34, CD45, CD29, CD44, and phycoerythrin-conjugated CD90, CD11b, and CD105 (all from BD Biosciences, Pharmingen). Nonspecific fluorescence and cell morphological features were determined by incubation with isotype-matched mouse monoclonal antibodies (BD Pharmingen). Positive cells were analyzed from at least 1×10^4 events collected and analyzed by flow cytometry with a FAC scan flow cytometer (BD Biosciences). Cellular phenotyping and multidifferentiation, as well as CFU-f were also tested as described previously [39].

Cell preconditioning and exposure to stress conditions

Passage 2 BM-MSCs were first starved in DMEM with 2% FBS overnight, and then preconditioned with DMEM supplemented with various concentrations of PRCR (0.1%, 1%, 10%, 20%) in 10% FBS or serum-free medium (SFM, StemPro® MSC SFM; Invitrogen) for 1, 3, 5, or 7 days. At each time point, cells were first starved in DMEM for 8 h, and then treated with different concentrations of hydrogen peroxide (H_2O_2) (0.1, 1, 10, 50, 100 μM/mL) for 8 h to induce stress. Apoptosis was assayed by using the Apoptosis APO-Percentage Assay Kit with a cellular dye that detected membrane alterations (phosphatidylserine flip) and stained apoptotic cells (Accurate Chemical & Scientific Corporation), which were then assayed on a colorimetric plate reader (Bio-Rad). Apoptotic cells were further stained in a terminal deoxynucleotidyl transferased UTP nick-end labeling (TUNEL) assay (In Situ Cell Death Detection Kit Fluorescein and TMR red; Roche Applied Science, GongChang.com). Cell survival was determined by trypan blue exclusion. For the detection of the active form of Ser-136 phosphorylated Bad and Bcl-xl, protein lysates were prepared and detected by western blot analysis and confocal imaging.

Preparation of conditioned medium

MSCs were first cultured in SFM (Gibco) with or without 10% PRCR preconditioning for 24 h, and then exposed to either normal or stress conditions (10 μM/mL H_2O_2) for 8 h to prepare conditioned medium (CM) (PRCR/MSC-CM and MSC-CM). Half of the CM was used to measure the secreted factors VEGF and PDGF. SFM and PRCR were also tested for these factors to determine the baseline levels of VEGF and PDGF. The other half of the CM was used to supplement the basal medium for the tube formation assay of HAECs. The collected culture supernatant was centrifuged at 1,500 rpm for 10 min and either used immediately or stored at −20°C.

Assays of platelet-derived growth factor receptor and cytokines

The same cell samples were used to measure mRNA and protein expression of platelet-derived growth factor receptor (PDGFR)-α by reverse transcription–polymerase chain reaction (RT-PCR) and western blot. The levels of VEGF, PDGF in culture supernatants were measured by RT-PCR and a Quantikine ELISA kit (R&D Systems) according to the manufacturer's instructions (www.rndsystems.com).

In vitro tube formation assay

The in vitro capillary morphogenesis assay was performed in 96-well plates coated with Matrigel (BD Biosciences), which had been pipetted (50 μL 10–12 mg/mL) into the culture wells and polymerized for 30–60 min at 37°C. HAECs incubated in basal medium supplemented with CM prepared as before were plated at 4×10^4 per cm^2 in triplicate and incubated under stress conditions. The plates were photographed at 6 and 24 h. The capillary morphology was examined with a Leica TCS SP5 confocal laser scanning microscope (Leica Microsystems) and further quantified by measuring the percentage field occupancy of capillary projections, as determined by image analysis. Six to nine photographic fields from three plates were scanned for each time point.

RNA purification and cDNA synthesis and PCR

BM-MSCs at passage 2 were seeded at 1×10^6 per cm^2 on tissue culture plastic, followed by exposure to 10% PRCR, 10% FBS, or SFM preconditioning for 24 h or 7 days under normal or stress conditions. Total RNA was extracted using Trizol reagent (Invitrogen) according to the manufacturer's instructions. cDNA was prepared using the Super Script First-Strand synthesis system (Invitrogen) and oligo-dT primers. The PCR mix consisted of 13 μL sterile deionized water, 2.5 μL *Taq* buffer, $MgCl_2$ (final concentration 2.5 mM), 0.28 mM dNTPs, 0.4 μM of each primer, 1.5 U *Taq* DNA polymerase (5 U/μL; Fermentas) and 4 μL of cDNA. The PCR program for both pairs of primers was as follows: 94°C for 2 min, followed by 33 cycles of 94°C (30 s), 58°C (30 s), and 72°C (30 s) for denaturation, annealing, and extension, respectively. PCR products were analyzed by electrophoresis in 1.5% agarose gel and visualized by UV fluorescence after staining with ethidium bromide. The images were captured by the built-in camera of the Molecular Imager Gel Doc™ XR+ System (Bio-Rad) under UV light. PCR amplification was performed using the primer sets shown in Supplementary Table S1 (Supplementary Data are available online at www.liebertpub.com/scd). The relative amount of each transcript in each sample was normalized to the reference gene *β-actin*, which was utilized as a loading control.

Western blot analysis

BM-MSCs at passage 2 were preconditioned with 10% PRCR, 10% FBS or SFM for 24 h or 7 days under normal or

stress conditions. Thereafter, proteins from the cell samples were extracted with cell lysis buffer (NP40 Cell Lysis Buffer; Life Technologies, Invitrogen), and then quantified with a Bicinchoninic Acid protein assay kit (Thermo Fisher). The proteins were then subjected to SDS-PAGE and transferred to a PVDF membrane (Millipore) using a semidry electroblotting system. After blocking the membrane with 5% skim milk in PBS, which was substituted with buffer containing goat serum when detecting the phosphorylated protein, the membranes were incubated with diluted primary antibodies, including rabbit polyclonal anti-rat antibodies to *PI3 kinase p85*, phosphorylated *PI3 kinase p85*, *AKT1*, *Ser-473* phosphorylated *AKT-1*, *NF-κB* and anti-rat antibodies to *Bcl-xl*, *Ser-136* phosphorylated *Bad* (1:1,000 dilution; from EPITOMICS, Abcam) and PDGF, VEGF, PDGFR-α, phospho-PDGFR-α, *β-actin* (1:1,000 dilution) (all from Abcam) at 4°C overnight. After washing with tris-buffered saline solution containing 0.1% Tween 20 [Tris-Buffered Saline Tween (TBST), Bio-Rad], the membrane was coincubated for 1 h with a 1:2,000 dilution of goat anti-rabbit biotin secondary antibody and a 1:2,000 dilution of the alternate goat anti-rabbit alkaline phosphatase secondary antibody in 10 mL of WesternDot™ blocking buffer (WesternDot 625 Goat Anti-Rabbit Western Blot Kit; Life Technologies, Invitrogen). After washing again with TBST, the protein bands were detected by chemiluminescence (1:2,000; Santa Cruz Biotechnology) and visualized using enhanced chemiluminescence (Pierce) with exposure to x-ray film. Relative optical densities of the protein bands were measured after subtracting the film background. Protein levels were normalized to β-actin, which was considered the loading control.

Immunocytochemistry and confocal laser scanning microscopy

For detection of the survival factors VEGF, PDGF, and PDGFR-α, *AKT*, *NF-κB* and *Bad*, cells at passage 2 preconditioned with 10% PRCR, 10% FBS or SFM for 24 h or 7 days under normal or stress conditions were grown to semi-confluence on glass coverslips, fixed in 3.7% buffered paraformaldehyde for 15 min and permeabilized with 0.1% Triton X-100 in PBS for 30 min. After using goat serum (Beyotime) to block nonspecific antigens for 1 h, the cells were incubated overnight with the following primary rabbit anti-rat antibodies: PDGF, VEGF, PDGFR-α (1:100; Abcam), *AKT*, *NF-κB*, and *Bad* (1:100; EPITOMICS, Abcam). FITC and DyLight® 488-conjugated goat anti-rabbit IgG (1:500; Santa Cruz Biotechnology) used as secondary antibodies were incubated with cells at 37°C for 1 h. Staining of 40, 6-diamino-2-phenylindole (DAPI) (Sigma-Aldrich) was used to visualize all nuclei. Finally, MSCs were examined with a Leica TCS SP5 confocal laser scanning microscope. Series of optical sections (1,024×1,024 pixels each) at intervals of 0.8 μm were obtained and superimposed to create a single composite image for each sample.

Subsequently, we pretreated BM-MSCs with 20 mM Tyrphostin AG1295 (PDGFR inhibitor; Sigma-Aldrich), 30 mM LY294002 (PI3K inhibitor; Cell Signaling Technology) 30 mM SC-66 (AKT inhibitor; Sigma-Aldrich), and neutralizing antibodies against VEGF (MAB564) and PDGF-AA (MAB1055) (final concentration, 10 μg/mL; R&D Systems) separately or together for 1 h before conducting all of the above experiments again. The optimal concentration of these inhibitors used in our study was firstly adjusted by the lactate dehydrogenase (LDH) Cytotoxicity Assay (www.sciencellonline.com) (data not shown).

Wound model and cell transplantation

Male Sprague–Dawley rats (250–300 g, 6–10 weeks old) were anesthetized with xylazine (20 mg/kg) and ketamine (100 mg/kg). A 2.0×2.0 cm sized and full-thickness skin defect was created on the back of each rat with surgical scissors. The wounds were treated once with 10^6 GFP-rat BM-MSCs (RAWMX-01101; Cyagen) in a total of 200 μL (5×10^6/mL) with or without PRCR preconditioning (group 1 or group 2) for 3 days by direct injection into the wound margins or wound bed. Wounded skin of the control group was untreated (group 3). The wounds were covered with polyurethane film (Department of Plastic Surgery, Guangzhou General Hospital, GuangDong), which was changed every 3 days when monitoring the wound condition and area.

Evaluation and quantification of surviving transplanted GFP-positive BM-MSCs

For monitoring survival of transplanted cells, we first tested the GFP signal intensity by in vivo optical imaging (Xenogen IVIS® Kinetic) (www.amv-europe.com/preclinical/products/in-vivo-imaging-systems/ivis-kinetic.html) on days 1, 3, 7, 12, and 22 post-transplantation. The animals were then sacrificed by cervical dislocation, and the wound tissues were sampled in full thickness, including the underlying muscle. Thereafter, samples were immediately processed for histological analysis. For the detection of GFP-positive cells, sections were embedded in OCT compound (Tissue-Tek 4583; Sakura Finetek), cut into 5-μm-thick sections at −22°C and subjected to antigen retrieval using 10 mM citrate buffer (pH=6) for 1 h at 95°C. After 3×5 min washes in PBS, sections were extracted for 20 min with 0.5% Triton X-100 in PBS on ice followed by 3×5 min washes in PBTC (PBS, 0.1% Na-Casein, 0.05% Tween-20, 0.1% fish gelatin), and then the fluorescently analyzed for GFP expression. Transplanted GFP-positive cells were counted at each time point on five serial coronal sections per skin (2 mm apart) using unbiased computational stereology.

Half of each specimen from day 7 was used for immunohistochemistry, and the other half was used for tissue TUNEL staining. For the histological analysis, specimens were fixed in formalin, washed 3×5 min in PBS at room temperature, dehydrated through a graded ethanol series (70%, 80%, 90%, 95%, 95%, 100%, and 100%) and finally incubated for 30 min in toluene. Thereafter, tissue samples were embedded in paraffin (Carl Roth) according to standard procedures. The samples were sectioned transversely at a thickness of 4 μm and incubated with the following primary antibodies overnight at 4°C: rabbit anti-rat *p-AKT1*, *p-PI3K* and *NF-κB* (1:100; EPITOMICS, Abcam). Horseradish peroxidase-coupled goat anti-rabbit IgG (1:1,000; Santa Cruz) was used as the secondary antibody and incubated with samples for 2 h at room temperature followed by light microscope analysis (KS400; Zeiss). Apoptotic cell death was detected by TUNEL staining using an In Situ Cell Death Detection Kit (TMR red; Roche Applied Science) according to the manufacturer's instructions.

Measurement of wound size and analysis of microscopic tissue regeneration

The macroscopic wound areas were quantified using photographs taken at various time points (day 1, 4, 8, 12, 16, 20, and 22) by tracing the wound margin and calculating the pixel area in relation to a ruler with a fine resolution computer mouse. The wound area was calculated as follows: wound area = percentage of the initial wound area − [wound area at specific time point]/[initial wound area] × 100%). Microscopic tissue regeneration was determined on Masson's trichrome-stained tissue sections by light microscope observation. Morphometric analysis was performed on digital images using the imaging software Image Pro Plus × 6.0 (Media Cybernetics).

Measurement of blood vessel density and epithelial regeneration and paracrine factors

Sections were made from frozen tissue samples collected on days 7 and 22 for immunohistochemical staining. Briefly, samples were embedded in OCT compound and cut into 10-μm-thick sections at −22°C. To stain regenerated arterioles, epidermis and paracrine factors, sections were incubated with mouse anti-rat α-smooth muscle actin (α-SMA) and VEGF antibodies or rabbit anti-rat CK5 and PDGF antibodies (all from Abcam) after fixation in ice methanol for 1 h and permeabilized with 0.1% Triton X-100 in PBS for 30 min. Subsequently, sections were incubated in Alexa Fluor 488-conjugated donkey anti-mouse and FITC-conjugated donkey anti-rabbit IgG (catalog no.A21206 and no.A31571, respectively; Invitrogen) at 37°C for 2 h. The sections were counterstained with DAPI and examined by fluorescence microscopy (Olympus). Ten slides were randomly selected from the middle part of each sample for analysis.

Statistical analysis

Either repeated measures analysis of variance (ANOVA) or two-way ANOVA with Bonferroni corrections where appropriate was used to test the probability of significant differences on parametric data, and the Kruskal-Wallis test with post hoc Dunn's testing between groups was performed for nonparametric data. Data are presented as the mean ± standard error of the mean from at least four independent experiments. $P < 0.05$ was considered statistically significant.

Results

Characterization of rat BM-MSCs

Culture-expanded confluent BM-MSCs displayed characteristic plastic adherence and spindle-shaped properties, and no significant differences in morphology or the immune phenotype were observed among the three groups. Their purity as determined by staining for various surface markers was 99.53% for CD29, 98.85% for CD90 and 97.84% for CD105. Among these hematopoietic stem cells in the PRCR group, contaminating population positive for CD11b, CD45, and CD34 were detected at frequencies of 0.10%, 0.13%, and 0.03%, respectively. Cultured BM-MSCs also had a strong CFU-f frequency and multiple differentiation functions, such as adipogenesis and osteogenesis (Supplementary Fig. S1A–C).

PRCR preconditioning promotes cell viability and reduces apoptosis of BM-MSCs under stress conditions

To determine the effect of PRCR on survival and apoptosis of BM-MSCs under stress conditions, we first determined that 10 μM/mL H_2O_2 was the optimal concentration for induction of stress condition by using the LDH Cytotoxicity Assay (www.sciencellonline.com) (data not shown). We found no significant differences between the effects of 10% PRCR and 20% PRCR on survival and apoptosis across the various tested time points. The APOPercentage assay revealed that after stress induction cellular apoptosis was apparent in each group compared with the normal condition, and PRCR preconditioned BM-MSCs (10% and 20%) had a significant reduction in the death rate compared with other groups (Fig. 1A). These results were also confirmed by the trypan blue exclusion assay (Fig. 1B), as well as by TUNEL immunofluorescence staining (Fig. 1C1, C2). Moreover, western blotting and fluorescent staining revealed lower Bad but increased Bcl-xl expression in PRCR preconditioned BM-MSCs compared with the other groups (Fig. 1D1, D2) on day 7.

We chose the optimal concentration of 10 μM/mL H_2O_2 and 10% PRCR for use in the following experiments.

PRCR preconditioning enhances PDGFR-α expression in rat BM-MSCs under stress conditions

We preconditioned BM-MSCs with PRCR, FBS and SFM for 24 h or 7 day without culture medium change. While PDGFR-α expression was enhanced by stress induction in all groups, the PRCR preconditioned BM-MSCs showed significantly higher levels of this gene compared with other groups (Fig. 2A). Moreover, the expression was increased at day 7 compared with that at 24 h and reached peak levels at day 7 under stress conditions in the PRCR group. The results were further supported at the protein level by western blot analysis (Fig. 2B). Additionally, subcellular detection by laser scanning confocal microscopy found PDGFR-α to be localized in the plasma membrane of the MSCs and enhanced by stress induction (Fig. 2C–E).

PRCR preconditioning enhances VEGF and PDGF secretion by BM-MSCs

Because PDGF and VEGF are implicated in the recruitment of MSCs at sites of injury or participation in angiogenesis, vascular remodeling and fibrosis after tissue wounding, we evaluated whether PRCR preconditioning could change the expression of these proteins in BM-MSCs under stress conditions in vitro. Significantly higher mRNA expression of VEGF and PDGF were detected in PRCR preconditioned BM-MSCs after stress stimulation compared with untreated BM-MSCs, while a mild change was observed under normal conditions between the two groups (Fig. 3A). Confocal images provided visual confirmation of these changes (Fig. 3B), and the levels of PDGF and VEGF measured by sandwich ELISA quantitatively demonstrated that both factors were significantly increased by PRCR preconditioning compared with untreated BM-MSCs alone after stress induction. Since the initial levels of these factors (PDGF and VEGF) in PRCR and SFM were identical and much

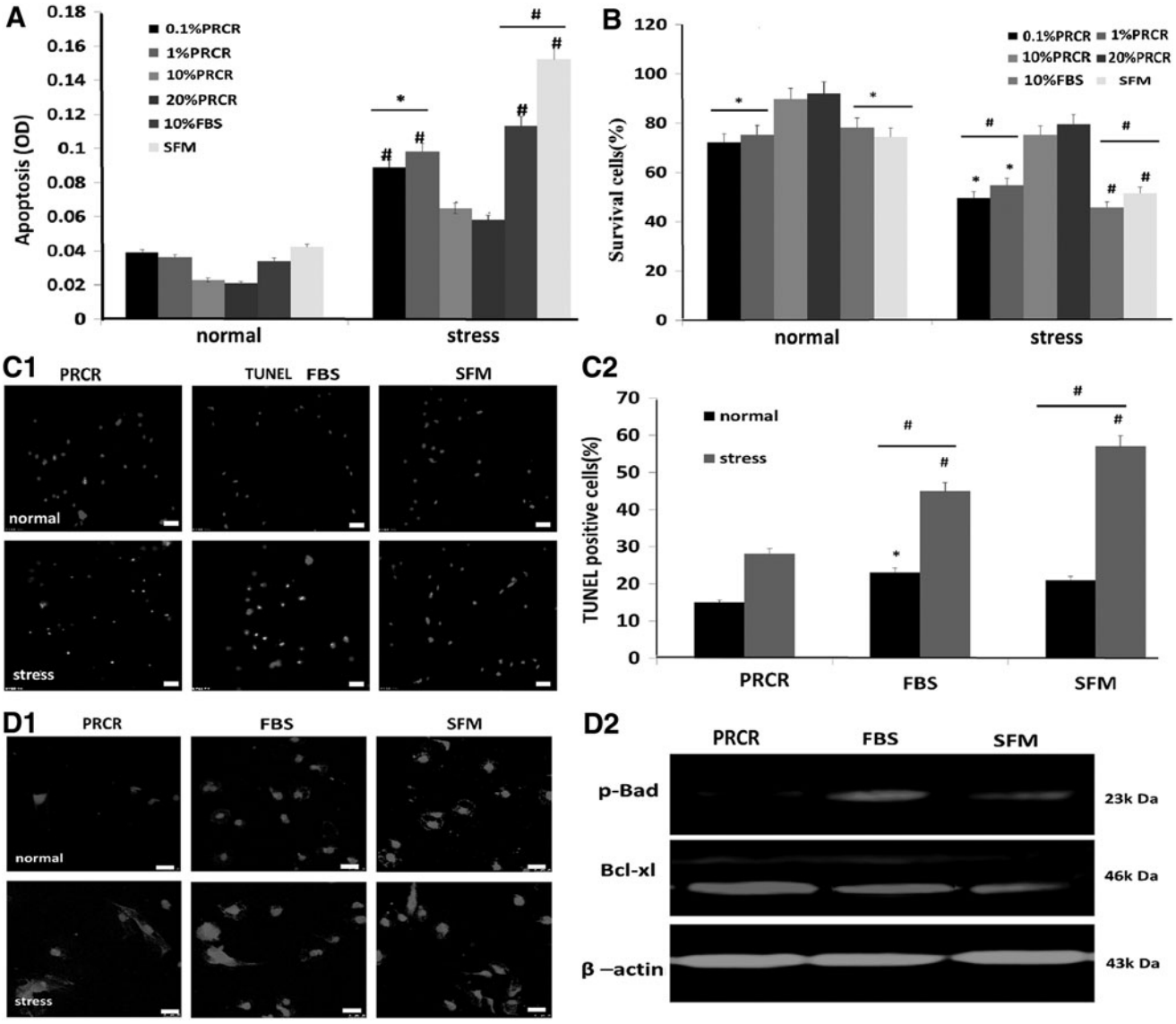

FIG. 1. Reduction of BM-MSC death by PRCR preconditioning in vitro. **(A)** APOPercentage assay results showing significantly decreased apoptosis in 10% and 20% PRCR groups under stress conditions. **(B)** Trypan blue assay results showing significantly increased cell viability in the PRCR group, compared with other groups under stress conditions. **(C1, C2)** TUNEL and DAPI staining showing obviously lower levels of positively stained cells in the PRCR group. **(D1, D2)** Western blotting assays and confocal microphotographs displaying lower levels of *Bad/Bcl-xl* in the PRCR group compared with other groups. Scale bar = 25 μm. DAPI (nucleus); Bad (cytoplasm). **(A, B, C2)** ($n = 4$),$^{*}P < 0.05$, $^{\#}P < 0.01$ versus 20% and 10% PRCR groups or versus normal conditions; **(C1)** scale bar = 25 mm. BM-MSCs, bone marrow-derived mesenchymal stem cells; MSCs, mesenchymal stem cells; PRCR, platelet rich clot releasate; TUNEL, terminal deoxynucleotidyl transferased UTP nick-end labeling.

lower than those of our experimental groups, their contribution to the paracrine molecules secreted by MSCs would be negligible (Fig. 3C1, C2).

Paracrine factors of VEGF and PDGF contribute to antiapoptotic and angiogenic effects of PRCR preconditioning on BM-MSCs under stress conditions

Because the survival factors VEGF and PDGF were reported to protect cells and promote angiogenesis in various cells, we investigated whether they accounted for antiapoptotic and angiogenic effects of PRCR preconditioning on BM-MSCs under hostile conditions. We pretreated PRCR preconditioned BM-MSCs (7 days) with control or blocking antibodies to VEGF and PDGF (separately or combined) before stress induction for 8 h. Neutralizing antibodies significantly decreased the antiapoptotic effects of PRCR preconditioning, as assayed using the APOPercentage kit, especially when combined together (1:1 volume) (Supplementary Fig. S2A1). Trypan blue exclusion assays also confirmed these results (Supplementary Fig. S2A2).

In the presence of Matrigel alone (growth factors reduced), HAECs under stress conditions did not initiate tube

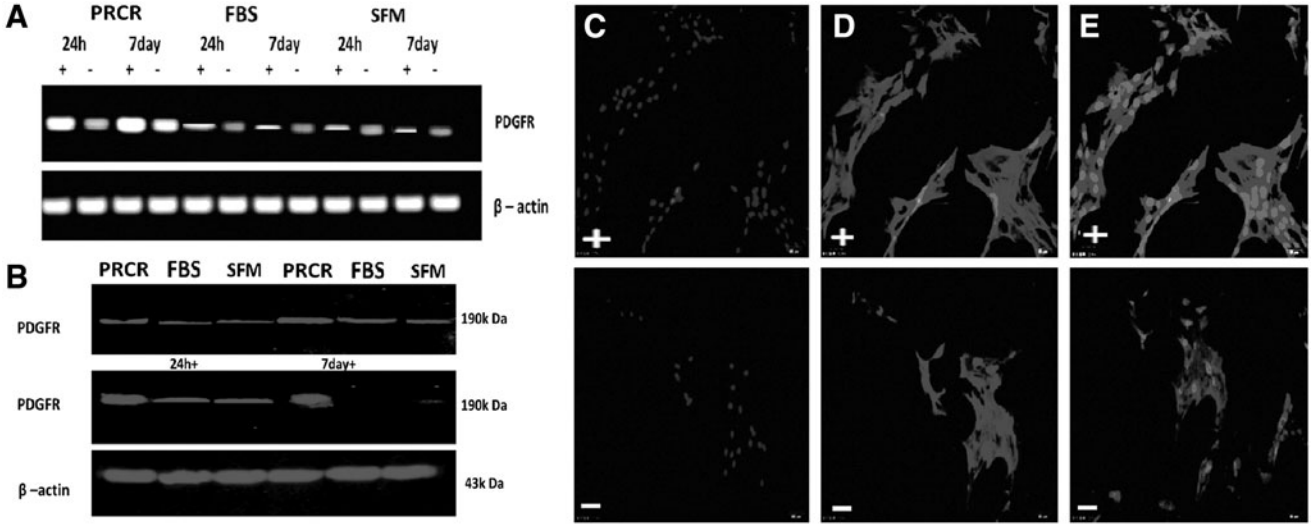

FIG. 2. PRCR preconditioning enhances PDGFR-α expression in BM-MSCs. **(A)** RT-PCR analysis showing enhanced PDGFR-α (296 bp) expression by stress induction in all groups and higher expression in the PRCR group compared with other groups. **(B)** Western blot analysis confirming the RT-PCR results. (PDGFR-α,190 kDa). **(C–E)** Subcellular localization of PDGFR-α in PRCR preconditioned MSCs. PDGFR and nuclei (DAPI) were stained. PDGFR was localized predominantly to the plasma membrane of MSCs **(E)**. (Scale bar = 25 μm). PDGFR positive cells in the total cells were 90.08% in the PRCR group, which was significantly higher than the other two groups (data not shown) ($n = 4$; three random fields per well). "+" indicates under stress conditions (10 μM/mL H_2O_2 and serum deprivation), "–" indicates without stress induction. H_2O_2, hydrogen peroxide; PDGF, platelet-derived growth factor; PDGFR, platelet-derived growth factor receptor; RT-PCR, reverse transcription–polymerase chain reaction.

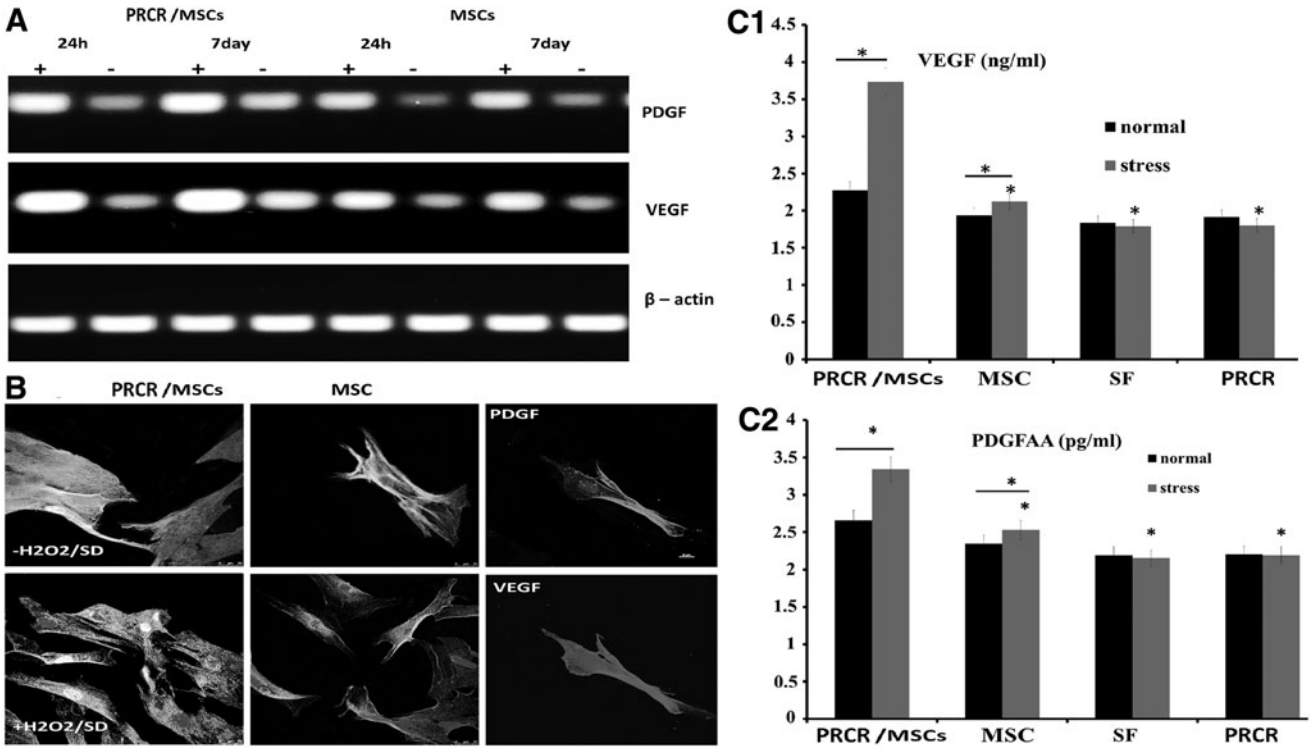

FIG. 3. Induction of paracrine factors from MSCs by PRCR preconditioning. **(A)** RT-PCR ($n = 4$) showing that PRCR preconditioned MSCs expressed higher mRNA levels of VEGF and PDGF, especially at day 7 under stress conditions. "+" indicates under stress conditions (10 μM/mL H_2O_2 and serum deprivation), "–" indicates without stress induction. **(B)** Confocal microscopy images confirming the RT-PCR results. VEGF, PDGF and nuclei (DAPI) were stained. Scale bar = 25 μm. **(C1, C2)** ELISA analysis of PDGF and VEGF ($n = 4$); $^*P < 0.01$ versus normal conditions or PRCR-MSC group. VEGF, vascular endothelial growth factor.

formation. In contrast, supplementation of the basal medium with CM with or without PRCR preconditioning stimulated tube formation after 6 h (data not shown). By 24 h, the HAECs had formed an interconnected network with a honeycomb appearance in all groups; in particular, HAECs cultured with PRCR/MSC-CM showed a robust vascular configuration and expression levels of VEGF and α-SMA (Supplementary Fig. S2B1). However, pretreatment of cells with neutralizing antibodies significantly reduced the angiogenic effects of PRCR/MSC-CM on HAECs (Supplementary Fig. S2B2). Quantification of the angiogenic effects further confirmed the results (Supplementary Fig. S1B3).

PRCR preconditioning upregulates survival genes PI3K *and* AKT1 *and activates downstream targets of* NF-κB

We next explored the mechanism underlying the cytoprotective effects of PRCR preconditioning on BM-MSCs. By RT-PCR analysis, PRCR preconditioning was shown to upregulate expression of *AKT1*, *PI3K*, and *NF-κB* significantly after stress induction compared with other groups, whereas those levels under normal conditions were just slightly higher in the PRCR group. Moreover, the expression of these signaling genes in the PRCR group seemed to be enhanced at day 7 compared with those at 24 h (Fig. 4A). This finding was also supported by western blot analysis of whole MSC lysates (Fig. 4B). Confocal microscopic detection further confirmed the enhanced cytoplasmic location of *AKT* and *NF-κB* in PRCR preconditioned cells (Fig. 4C). To verify the role of *PI3K/AKT/NF-κB* signaling pathways on PRCR preconditioning, we pretreated MSCs with LY294002, SC-66 or AG1295 for 1 h before PRCR preconditioning. These inhibitors reversed PRCR preconditioning induced expression of *PI3K*, *AKT1*, and *NK-κB* at both the gene and protein levels in MSCs (Fig. 4D). Meanwhile, only low or even undetectable levels of phosphorylated *JNK* and *MAPK* were constitutively present in MSCs with PRCR preconditioning under normal or stress conditions, and the addition of the above inhibitors did not change their levels (data not shown). These results suggested that the *PI3K-AKT* pathway activated by PRCR preconditioning was not targeting the *JNK*/transcriptional (*STAT*) and extracellular signal-regulated kinase (*ERK*)/*MAPK* pathway.

PDGFR-α/PI3K/AKT1 *signaling pathways contribute to PRCR-mediated effects on BM-MSCs in vitro*

We next examined the biological sequelae of *AKT1* activation in MSCs with PRCR preconditioning. Specifically, the effects of AG1295, LY294002, and SC-66 on the cytoprotection, paracrine factors, and tube formation induced by PRCR preconditioning were determined. MSCs were preincubated with these inhibitors separately for 1 h before preconditioning with PRCR (24 h), and then exposed to stress conditions for 8 h. AG1295, LY294002 and SC-66 significantly decreased VEGF and PDGF expression induced by PRCR preconditioning in MSCs. Treatment with these inhibitors also reversed the PRCR induced antiapoptotic effects, tube formation by HAECs, as well as PDGFR expression (data not shown). However, no effects on apoptosis, paracrine factors, and tube formation were observed with the *MAPK* inhibitor (PD98059, 50 μM) of *ERK* signaling (data not shown).

PRCR preconditioning reduces death of transplanted BM-MSCs in vivo

At 6 h after transplantation of GFP-BM-MSCs into the ischemic wound, we investigated whether PRCR preconditioning could protect the grafted cells from acute injury in vivo. When BM-MSCs without PRCR preconditioning were transplanted into the ischemic subcutaneous tissue, GFP signals decreased remarkably 2 h after transplantation, while this signal was only slightly decreased with PRCR preconditioning. Moreover, the signals in PRCR group were significantly higher at all detected time points compared with the control group (Fig. 5A). We next counted the number of TUNEL-positive grafted cells in the wound skin at day 7 after transplantation and found that PRCR preconditioning reduced it by 53.6% (Fig. 5B, C). Furthermore, on days 1, 3, 7, 12, and 22 of the experiment, sections were prepared from every 2 mm of the tissue specimen to count the number of GFP-positive cells. We found that PRCR preconditioning significantly increased survival of the grafted cells at all detected time points (Fig. 5D). Taken together, the results showed that PRCR preconditioning protected the grafted MSCs from death in a hostile host skin environment.

PRCR preconditioning strengthens wound repair and skin tissue regeneration of BM-MSCs

The wound closure area at each detected time point was expressed as a percentage of the original wound size. At each detected time point, healing was significantly more rapid in group 1 compared to the other groups. The wound was nearly closed on day 16 in group 1, while there were gaps in the wounds of groups 2 and 3 until day 22 or beyond (Fig. 6A). Masson's trichrome staining of histological sections on day 12 indicated that the tissue architecture at the healing wound of group 1, which showed complete epithelialization and orderly collagen arrangement, was most similar to that of normal skin; meanwhile, in groups 2 and 3, there were still several millimeters of gaps between epithelial wound edges and the collagen was disarranged (Fig. 6B). Epithelial tissue repair was evaluated by immunofluorescent detection of rat CK5 at the midportion of the wound on days 7 and 22. Group 1 showed enhanced expression of CK5 compared with the other two groups, especially on day 22 when it was similar to that of normal skin, while the other two groups still showed low levels of CK5 expression (Fig. 6C). Immunofluorescent staining for rat α-SMA and quantification of blood vessel density revealed that blood vessel growth was significantly enhanced in group 1 compared with the other groups (Fig. 6D, E).

Potential mechanism of the positive effects of PRCR preconditioning on BM-MSCs before transplantation

Immunohistochemical analysis showed pronounced p-*PI3K*, *p-AKT1*, and *NF-κB* expression at the skin wound site

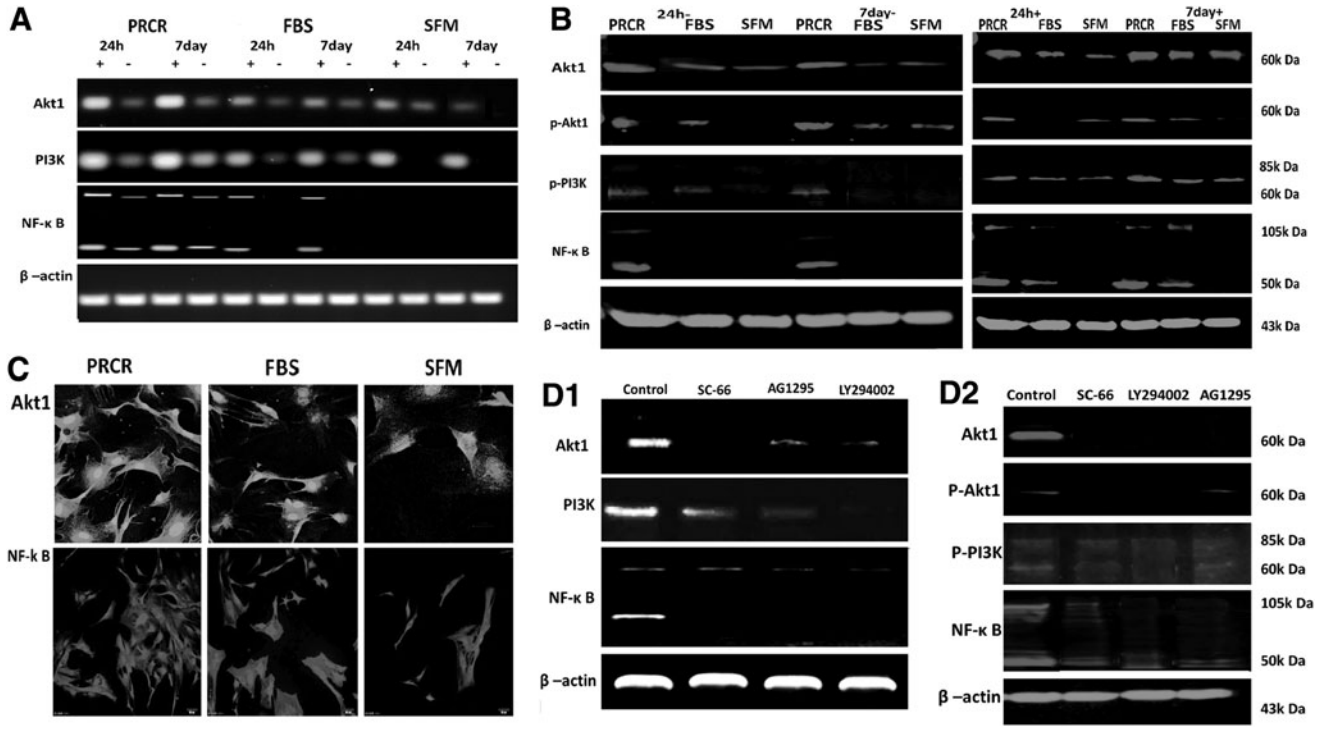

FIG. 4. Upregulation of survival genes in BM-MSCs with PRCR preconditioning in vitro. **(A)** RT-PCR analysis ($n=4$) revealing that preconditioning with PRCR induced significantly higher gene expression of *AKT1, PI3K, NF-κB* both at 24 h and day 7 compared with FBS and SFM groups. **(B)** Western blot analysis of whole cell lysate of MSCs ($n=4$) confirming the RT-PCR results. β-actin was used as an internal control. "+" indicates under stress conditions (10 μM/mL H_2O_2 and serum deprivation), "−" indicates normal induction. **(C)** Confocal microscopy displaying the enhanced *AKT1* and *NF-κB* cytoplasmic expression in the PRCR group. (Scale bar = 25 μm). **(D1, D2)** LY294002, AG1295 and SC-66 pretreatment reversed the enhancement of both gene and protein levels of *AKT, PI3K* and NF-κB by PRCR preconditioning. FBS, fetal bovine serum; SFM, serum-free medium.

of animals transplanted with PRCR preconditioned BM-MSCs compared with other groups on day 7 (Fig. 7B). We also measured and compared secreted proteins on days 7 and 22 in each group by immunofluorescent staining. The images showed significant upregulation of VEGF and PDGF in group 1 compared with the other two groups (Fig. 7A). These factors may be secreted by donor cells or the host cells and function through a paracrine or autocrine route.

Taken together, the in vivo results supported that the PRCR preconditioning enhanced the survival of grafted BM-MSCs and skin regeneration by upregulation of paracrine factors via the *PI3K/AKT/NF-κB* pathways. Of note, these in vivo findings coincided with those observed in vitro.

Discussion

PRCR–"a cytoprotective agent" to prevent rat BM-MSC apoptosis under hostile microenvironments

Currently, MSCs used in therapy are considered as site-regulated, multidrug dispensaries, or "drugstores" to promote and support the natural regeneration of focal injuries. However, graft survival remains a major challenge in cell-based therapy and is crucial for the success of transplantation therapy [40]. We have demonstrated in this study for the first time that PRCR preconditioned BM-MSCs not only showed a better survival rate but also expressed higher levels of paracrine factors, which resulted in stronger therapeutic effects on an acute wound. The major findings were: (i) PRCR preconditioning protected BM-MSCs from apoptosis under stress conditions in vitro or acute injury in vivo, and transplantation of the PRCR/BM-MSCs accelerated skin wound repair; (ii) PRCR preconditioning enhanced the paracrine secretions of BM-MSCs, and these factors contributed to the cellular protective and angiogenic properties of the HAECs; (iii) the mechanism of PRCR preconditioning enhanced self-protection, paracrine function, as well as skin repair or regenerative ability of BM-MSCs, which were at least, in part, due to activation of the PDGFR/*PI3K/AKT* signaling pathways and genes downstream of *NF-κB*; (iv) inhibition of this signaling pathways reversed the positive effects on BM-MSCs induced by PRCR preconditioning under stress conditions in vitro. The use of PRCR, which can be prepared with standard methods and contains an autogenous mix of various cytokines in biologically appropriate proportions, avoids the risks of exposure to xenogeneic compounds from animal products or gene modified agents. Therefore, we believe the beneficial effects of PRCR preconditioning, including induction of platelet growth factor release, allow transplanted MSCs to withstand the rigors of the host microenvironment. Along with their simplicity, ease of access and lack of safety issues, the benefits of MSCs make

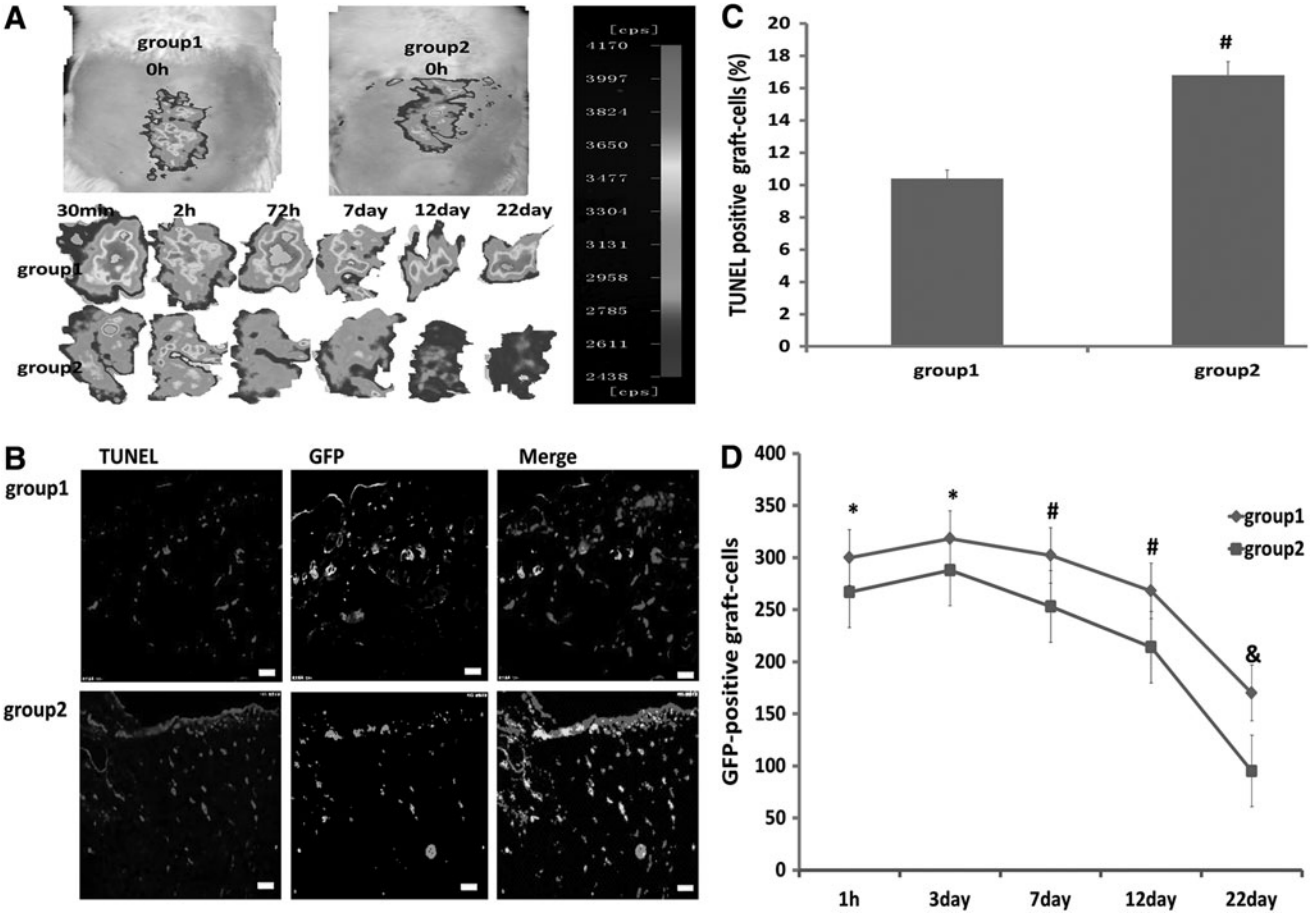

FIG. 5. Reduction of grafted BM-MSC death by PRCR preconditioning in vivo. **(A)** Optical in vivo imaging showing enhanced intensity and durability of GFP signals in PRCR group (group 1) compared with control group (group 2). **(B, C)** Representative figures of TUNEL staining at day 7 showing that PRCR preconditioning before transplantation significantly reduced the number of TUNEL-positive grafted cells. (Scale bar = 25 mm). ($n = 4$), $^{\#}P < 0.01$ versus group 1. **(D)** Quantification of the number of surviving grafted cells at 22 days after transplantation and injury. PRCR preconditioning significantly increased the survival of grafted MSCs ($n = 4$); $^{*}P < 0.05$, $^{\#}P < 0.01$, $^{\&}P < 0.001$ versus group 1.

this approach highly appealing for the future development of widely available autologous biomaterials (MSCs and other stem cells) for therapeutic clinical applications (Supplementary Fig. S3).

PDGFR dependent autocrine/paracrine loops of VEGF and PDGF are important for self-protective and regenerative functions of BM-MSCs

Paracrine secretions of MSCs were reported more than 15 years ago when Haynesworth et al. described their synthesis of a broad spectrum of growth factors, chemokines and cytokines, such as VEGF, PDGF, fibroblastic growth factor, hepatocyte growth factor, and stromal cell-derived factor-1, which exert effects on the MSCs themselves and other cells in their vicinity [41]. These factors have been postulated to promote arteriogenesis [42], support the stem cell crypt in the intestine [43], protect against ischemic renal injury [44] and maintain hematopoiesis [45]. They have also been known to provide beneficial effects on the heart, including neovascularization [46,47] and attenuation of ventricular wall thinning [48]. Previous studies have attributed the angiogenic function of PRP to PDGF and VEGF [49], and the interaction between PDGF and PDGFR is key for the survival of many cells [50]. Specifically, PDGFR is reported to play pivotal roles by transducing extracellular stimuli to intracellular signaling circuits via the PDGF/PDGFR axis to promote cellular growth and proliferation [51], as well as support pericyte/endothelial cell interplay and vasculature stability [52–54]. Inactivation of PDGF and PDGFR genes in embryonic stem cells is associated with cardiovascular, hematological and renal defects [55]. While a previous study found no VEGFR expression in MSCs [56], others have reported that VEGF can directly signal through PDGFR [57] and that activation of the VEGF autocrine loop in selected microenvironments contributes to optimal differentiation and survival of stem cells [58,59]. Here we proposed a novel VEGF-PDGF/PDGFR signaling mechanism for PRCR preconditioning induced autocrine/paracrine effects of VEGF and PDGF, which are important for cell survival and regenerative functions. This intriguing hypothesis is supported by our current findings: (i) we first

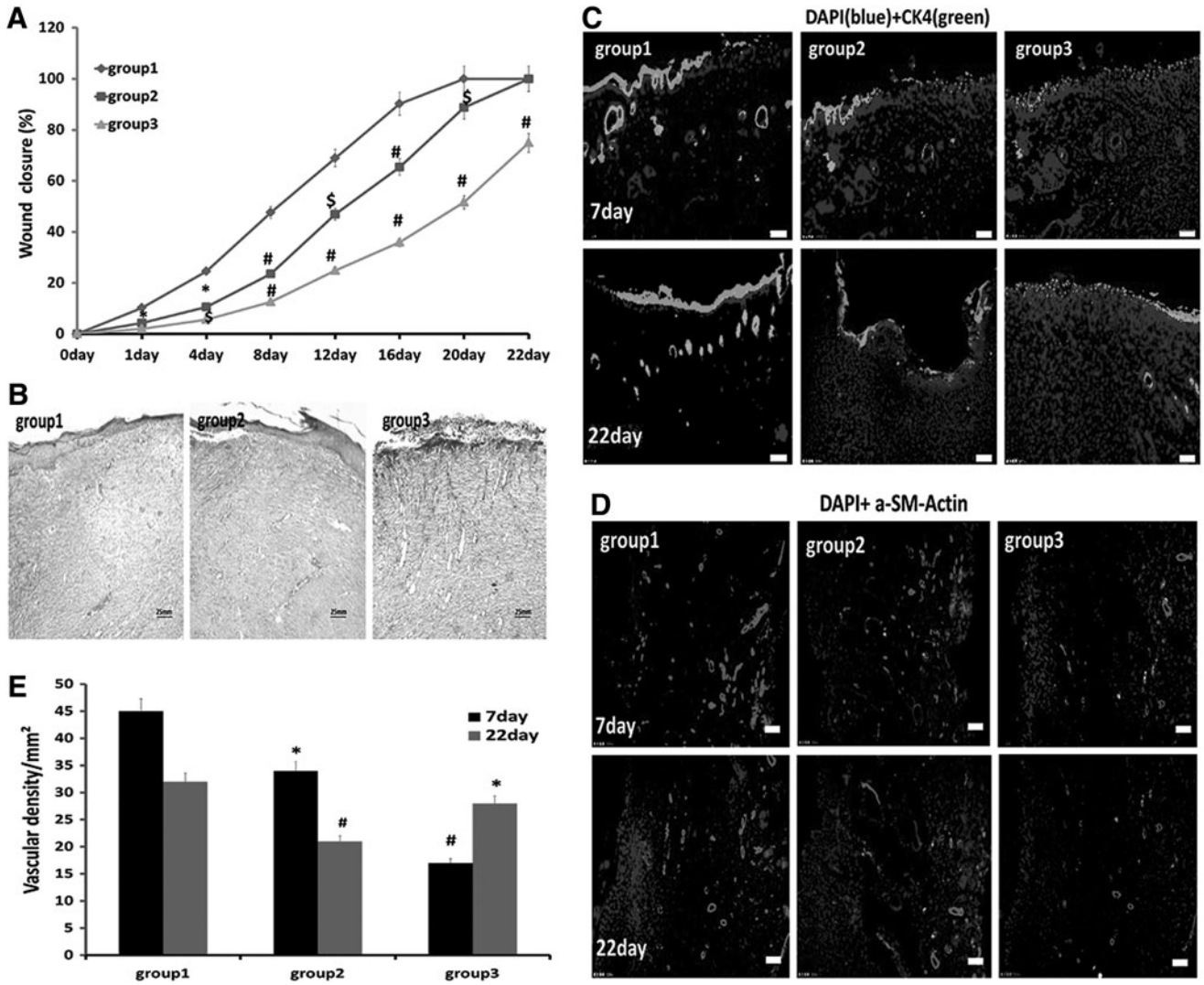

FIG. 6. PRCR preconditioned BM-MSCs improve wound closure and epithelization and blood vessel density. **(A)** Measurement of wound closure rates. Wound sizes were significantly decreased in group 1 compared with the other two groups ($n=6$); $^{*}P<0.05$, $^{\$}P<0.01$, $^{\#}P<0.001$ versus group 1. **(B)** Masson's Trichrome-stained sections of wounds on day 12 revealing that the grafted PRCR preconditioned MSCs enhanced wound regeneration. **(C, D)** Immunofluorescence staining of skin tissue sections on days 7 and 22 showing transplantation of PRCR preconditioned MSCs enhanced regeneration of the epidermis and blood vessels. (Scale bar = 25 mm). **(E)** Quantification of regenerated blood vessels to confirm immunofluorescence staining results ($n=4$), $^{*}P<0.05$, $^{\#}P<0.001$ versus group 1. α-SMA, α-smooth muscle actin.

demonstrated that VEGF and PDGF were enhanced by PRCR preconditioning in a hostile microenvironment; (ii) they were shown to be important for PRCR-induced antiapoptosis and angiogenesis in vitro, as well as for skin regeneration after transplantation in vivo; (iii) their expression were largely decreased when pretreated with AG1295 (PDGFR inhibitor), and the antiapoptosis and angiogenesis function were significantly inhibited by VEGF and PDGF blocking antibodies.

In light of earlier studies showing that ex vivo gene modification of stem cells for overexpression of various paracrine factors were cytoprotective, we anticipated that PRCR preconditioned stem cells, which are capable of releasing a multitude of prosurvival paracrine factors, would be more appealing.

PI3K/AKT/NF-κB *signaling pathways account for PRCR preconditioning effects on BM-MSCs*

Elucidation of the molecular pathways mediating MSCs secretions is a crucial step toward improving our understanding of the profile of secreted factors and their clinical utility. A wide array of signaling pathways has been implicated in paracrine-mediated repair by MSCs [60,61]. It is well established that interactions among PDGF, VEGF and PDGFR are key for the phosphorylation of PDGFR and activation of *PI3K*, which is the critical activator of *AKT* [62,63]. The phosphorylation of *AKT* then mediates metabolic, survival/apoptotic [64–66] and differentiation functions in a variety of cells, such as endothelial differentiation of mouse embryonic stem cells [67] and MSCs [68,69]. Furthermore, in

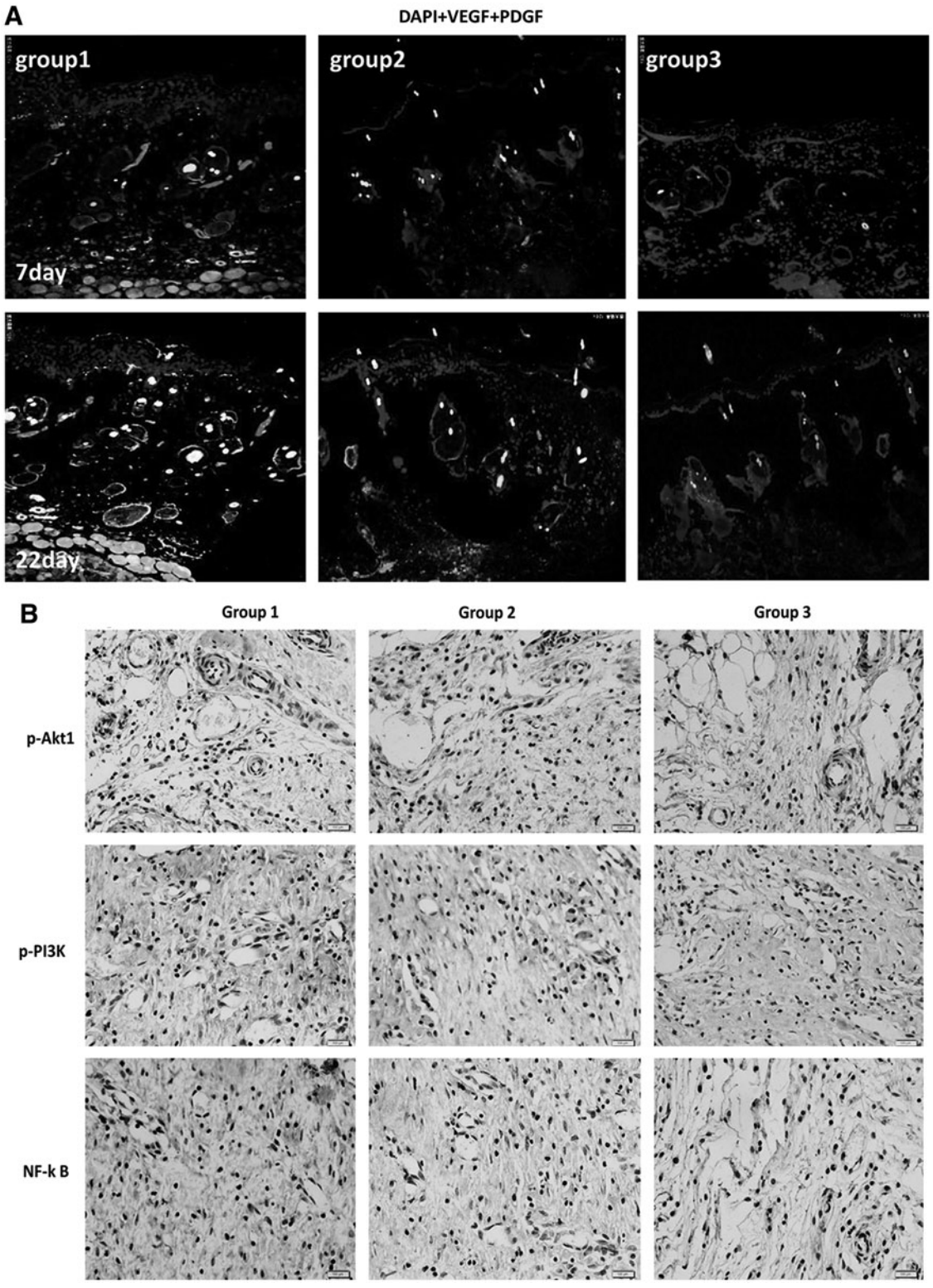

FIG. 7. Mechanism of PRCR preconditioned BM-MSCs enhancing skin regeneration. **(A)** Representative immunofluorescence images showing the enhanced VEGF and PDGF expression (with DAPI stained nuclei) in PRCR preconditioned MSCs treatment group on days 7 and 22 compared with other groups (scale bar = 25 mm). **(B)** Immunohistochemistry demonstrating higher levels of *p-PI3K, p-AKT1* and *NF-κB* expression in wound bed transplanted with PRCR preconditioned MSCs on day ($n = 4$), (scale bar = 25 mm).

the process of *NF-κB* activation, *p-AKT* activates the inhibitor of kappa B (*IκB*) kinase; thus, increasing *IκB* phosphorylation and degradation [70]. The activation of *NF-κB* is an important molecular event in regulating the expression of more than 150 target genes [71–73] that code for cytokines, chemokines, growth factors, cell adhesion proteins, as well as cell surface receptors. Deletion of the *NF-κB* (p65) subunit or expression of *IκB* inhibits the expression of several critical antiapoptotic proteins, including the specific inhibitor of *caspase-8*, cellular inhibitors of apoptosis (*cIAP1* and *cIAP2*), *Bcl-xl* [74] and the production of cytokines [75].

These studies enlighten us on the *PI3K/AKT/NF-κB* pathway, which is considered a central regulator of stress response and a key mediator of cell survival and immune responses. In our investigation, we demonstrated that PRCR preconditioning promoted survival genes involved in *AKT1* phosphorylation and canonical activation of *NF-κB* in MSCs, especially under hostile conditions, thereby enhancing the paracrine factors and skin regenerative functions of these cells. In addition, the cytoprotective effects induced by PRCR preconditioning may also occur through other mechanisms, including direct inhibition of *Bad* and selective upregulation of the antiapoptotic protein *Bcl-xl* [76–79]. However, since the enhanced paracrine factors and antiapoptotic effects induced by PRCR preconditioning were not completely inhibited by pretreatment with the inhibitors of PDGFR, *PI3K*, and *AKT*, other contributing factors may also be involved in the improvement of cytoprotective, paracrine and regenerative functions of MSCs. In fact, many of these growth factors, including TGF-β and IGF-I are also well-established antiapoptotic growth factors, and they were likely responsible, in part, for the PRCR-mediated effects. Future studies should further address these important tissues when using MSCs with PRCR preconditioning.

Conclusion

In summary, we have established that PRCR preconditioning can reprogram rat BM-MSCs to express higher levels of paracrine factors and tolerate hostile conditions, resulting in enhanced angiogenic effects in vitro and tissue regeneration functions in vivo. PRCR preconditioning of transplanted BM-MSCs may also facilitate their other functions, such as immunomodulation and cell replacement. In future studies, we will increase the number of samples and time points monitored, as well as utilize gene disruption or RNA interference techniques to further verify our observed effects of PRCR preconditioning on BM-MSCs. Furthemore, we will explore the intriguing "stemness preserved" atavism of MSCs by incorporating them into lyophilized porous PRCR film mixed with natural cellulose. This direction of research may bring new insights into both stem cell biology and tissue engineering.

Acknowledgments

This article was supported, in part, by the National Natural Science Foundation of China (81121004, 8123041, 81171812, 81000843, 81272105), the National Basic Science and Development Program (973 Program, 2012CB518105), Guangzhou City Science and Technology Project (10C36091671, 2012J4100044), Guangdong Provincial Science and technology projects (2009B080701092) and the Major National Science and Technology Programs (2011ZXJ09104-07C) funded by the CHINA government.

Author Disclosure Statement

No competing financial interests exist.

References

1. Caplan AI and D Correa. (2011). The MSC: an injury drugstore. Cell Stem Cell 9:11–15.
2. Kim SW, H Han, GT Chae, SH Lee, S Bo, JH Yoon, YS Lee, KS Lee, HK Park and KS Kang. (2006). Successful stem cell therapy using umbilical cord blood-derived multipotent stem cells for Buerger's disease and ischemic limb disease animal model. Stem Cells 24:1620–1626.
3. Ishikane S, S Ohnishi, K Yamahara, M Sada, K Harada, K Mishima, K Iwasaki, M Fujiwara, S Kitamura, et al. (2008). Allogeneic injection of fetal membrane-derived mesenchymal stem cells induces therapeutic angiogenesis in a rat model of hind limb ischemia. Stem Cells 26:2625–2633.
4. Dai W, SL Hale, BJ Martin, JQ Kuang, JS Dow, LE Wold and RA Kloner. (2005). Allogeneic mesenchymal stem cell transplantation in postinfarcted rat myocardium: short- and long-term effects. Circulation 112:214–223.
5. Amado LC, AP Saliaris, KH Schuleri, M St John, JS Xie, S Cattaneo, DJ Durand, T Fitton, JQ Kuang, et al. (2005). Cardiac repair with intramyocardial injection of allogeneic mesenchymal stem cells after myocardial infarction. Proc Natl Acad Sci U S A 102:11474–11479.
6. Hatzistergos KE, H Quevedo, BN Oskouei, Q Hu, GS Feigenbaum, IS Margitich, R Mazhari, AJ Boyle, JP Zambrano, et al. (2010). Bone marrow mesenchymal stem cells stimulate cardiac stem cell proliferation and differentiation. Circ Res 107:913–922.
7. Gnecchi M, Z Zhang, A Ni and VJ Dzau. (2008). Paracrine mechanisms in adult stem cell signaling and therapy. Circ Res 103:1204–1219.
8. Aggarwal S and MF Pittenger. (2005). Human mesenchymal stem cells modulate allogeneic immune cell responses. Blood 105:1815–1822.
9. Menasche P. (2008). Current status and future prospects for cell transplantation to prevent congestive heart failure. Semin Thorac Cardiovasc Surg 20:131–137.
10. Herberg S, X Shi, MH Johnson, MW Hamrick, CM Isales and WD Hill. (2013). Stromal cell-derived factor-1beta mediates cell survival through enhancing autophagy in bone marrow-derived mesenchymal stem cells. PLoS One 8:e58207.
11. Xu J, J Qian, X Xie, L Lin, Y Zou, M Fu, Z Huang, G Zhang, Y Su and J Ge. (2012). High density lipoprotein protects mesenchymal stem cells from oxidative stress-induced apoptosis via activation of the PI3K/Akt pathway and suppression of reactive oxygen species. Int J Mol Sci 13:17104–17120.
12. Savitz SI, DM Rosenbaum, JH Dinsmore, LR Wechsler and LR Caplan. (2002). Cell transplantation for stroke. Ann Neurol 52:266–275.
13. Lo EH, T Dalkara and MA Moskowitz. (2003). Mechanisms, challenges and opportunities in stroke. Nat Rev Neurosci 4:399–415.
14. Hodgetts SI, MW Beilharz, AA Scalzo and MD Grounds. (2000). Why do cultured transplanted myoblasts die in vivo? DNA quantification shows enhanced survival of donor male myoblasts in host mice depleted of CD4+ and CD8+ cells or Nk1.1+ cells. Cell Transplant 9:489–502.

15. Chacko SM, S Ahmed, K Selvendiran, ML Kuppusamy, M Khan and P Kuppusamy. (2010). Hypoxic preconditioning induces the expression of prosurvival and proangiogenic markers in mesenchymal stem cells. Am J Physiol Cell Physiol 299:C1562–1570.
16. Busletta C, E Novo, L Valfre Di Bonzo, D Povero, C Paternostro, M Ievolella, K Mareschi, I Ferrero, S Cannito, et al. (2011). Dissection of the biphasic nature of hypoxia-induced motogenic action in bone marrow-derived human mesenchymal stem cells. Stem Cells 29:952–963.
17. Wisel S, M Khan, ML Kuppusamy, IK Mohan, SM Chacko, BK Rivera, BC Sun, K Hideg and P Kuppusamy. (2009). Pharmacological preconditioning of mesenchymal stem cells with trimetazidine (1-[2,3,4-trimethoxybenzyl]piperazine) protects hypoxic cells against oxidative stress and enhances recovery of myocardial function in infarcted heart through Bcl-2 expression. J Pharmacol Exp Ther 329:543–550.
18. Lu C, D Chen, Z Zhang, F Fang, Y Wu, L Luo and Z Yin. (2007). Heat Shock Protein 90 regulates the stability of c-Jun in HEK293 Cells. Mol Cells 24:210–214.
19. Chen D, J Pan, B Du and D Sun. (2005). Induction of the heat shock response in vivo inhibits NF-kappaB activity and protects murine liver from endotoxemia-induced injury. J Clin Immunol 25:452–461.
20. Pasha Z, Y Wang, R Sheikh, D Zhang, T Zhao and M Ashraf. (2008). Preconditioning enhances cell survival and differentiation of stem cells during transplantation in infarcted myocardium. Cardiovasc Res 77:134–142.
21. Bartunek J, JD Croissant, W Wijns, S Gofflot, A de Lavareille, M Vanderheyden, Y Kaluzhny, N Mazouz, P Willemsen, et al. (2007). Pretreatment of adult bone marrow mesenchymal stem cells with cardiomyogenic growth factors and repair of the chronically infarcted myocardium. Am J Physiol Heart Circ Physiol 292:H1095–H1104.
22. Ye L, H Haider, S Jiang, LH Ling, R Ge, PK Law and KE Sim. (2005). Reversal of myocardial injury using genetically modulated human skeletal myoblasts in a rodent cryoinjured heart model. Eur J Heart Fail 7:945–952.
23. Azarnoush K, A Maurel, L Sebbah, C Carrion, A Bissery, C Mandet, J Pouly, P Bruneval, AA Hagege and P Menasche. (2005). Enhancement of the functional benefits of skeletal myoblast transplantation by means of coadministration of hypoxia-inducible factor 1alpha. J Thorac Cardiovasc Surg 130:173–179.
24. Kofidis T, JL de Bruin, T Yamane, LB Balsam, DR Lebl, RJ Swijnenburg, M Tanaka, IL Weissman and CR Robbins. (2004). Insulin-like growth factor promotes engraftment, differentiation, and functional improvement after transfer of embryonic stem cells for myocardial restoration. Stem Cells 22:1239–1245.
25. Gnecchi M, H He, OD Liang, LG Melo, F Morello, H Mu, N Noiseux, L Zhang, RE Pratt, et al. (2005). Paracrine action accounts for marked protection of ischemic heart by Akt-modified mesenchymal stem cells. Nat Med 11:367–368.
26. Jiang S, H Haider, NM Idris, A Salim and M Ashraf. (2006). Supportive interaction between cell survival signaling and angiocompetent factors enhances donor cell survival and promotes angiomyogenesis for cardiac repair. Circ Res 99:776–784.
27. Kutschka I, T Kofidis, IY Chen, G von Degenfeld, M Zwierzchoniewska, G Hoyt, T Arai, DR Lebl, SL Hendry, et al. (2006). Adenoviral human BCL-2 transgene expression attenuates early donor cell death after cardiomyoblast transplantation into ischemic rat hearts. Circulation 114: I174–I180.
28. Mei-Dan O, L Laver, M Nyska and G Mann. (2011). [Platelet rich plasma—a new biotechnology for treatment of sports injuries]. Harefuah 150:453–457, 490.
29. Kim DH, YJ Je, CD Kim, YH Lee, YJ Seo, JH Lee and Y Lee. (2011). Can platelet-rich plasma be used for skin rejuvenation? evaluation of effects of platelet-rich plasma on human dermal fibroblast. Ann Dermatol 23:424–431.
30. Fukaya Y, M Kuroda, Y Aoyagi, S Asada, Y Kubota, Y Okamoto, T Nakayama, Y Saito, K Satoh and H Bujo. (2012). Platelet-rich plasma inhibits the apoptosis of highly adipogenic homogeneous preadipocytes in an in vitro culture system. Exp Mol Med 44:330–339.
31. Kocaoemer A, S Kern, H Kluter and K Bieback. (2007). Human AB serum and thrombin-activated platelet-rich plasma are suitable alternatives to fetal calf serum for the expansion of mesenchymal stem cells from adipose tissue. Stem Cells 25:1270–1278.
32. Reinisch A, C Bartmann, E Rohde, K Schallmoser, V Bjelic-Radisic, G Lanzer, W Linkesch and D Strunk. (2007). Humanized system to propagate cord blood-derived multipotent mesenchymal stromal cells for clinical application. Regen Med 2:371–382.
33. Mishra A, P Tummala, A King, B Lee, M Kraus, V Tse and RC Jacobs. (2009). Buffered platelet-rich plasma enhances mesenchymal stem cell proliferation and chondrogenic differentiation. Tissue Eng Part C Methods 15:431–435.
34. Lin SS, R Landesberg, HS Chin, J Lin, SB Eisig and HH Lu. (2006). Controlled release of PRCR-derived growth factors promotes osteogenic differentiation of human mesenchymal stem cells. Conf Proc IEEE Eng Med Biol Soc 1:4358–4361.
35. Eppley BL, WS Pietrzak and M Blanton. (2006). Platelet-rich plasma: a review of biology and applications in plastic surgery. Plast Reconstr Surg 118:147e–159e.
36. Hu Z, SA Peel, SK Ho, et al. (2009). Platelet-rich plasma induces mRNA expression of VEGF and PDGF in rat bone marrow stromal cell differentiation. Oral Surg Oral Med Oral Pathol Oral Radiol Endod 107:43–48.
37. Bir SC, J Esaki, A Marui, K Yamahara, H Tsubota, T Ikeda and R Sakata. (2009). Angiogenic properties of sustained release platelet-rich plasma: characterization in-vitro and in the ischemic hind limb of the mouse. J Vasc Surg 50:870–879, e872.
38. Harichandan A and HJ Buhring. (2011). Prospective isolation of human MSC. Best Pract Res Clin Haematol 24:25–36.
39. Wang HS, SC Hung, ST Peng, CC Huang, HM Wei, YJ Guo, YS Fu, MC Lai and CC Chen. (2004). Mesenchymal stem cells in the Wharton's jelly of the human umbilical cord. Stem Cells 22:1330–1337.
40. Haider H and M Ashraf. (2008). Strategies to promote donor cell survival: combining preconditioning approach with stem cell transplantation. J Mol Cell Cardiol 45:554–566.
41. Haynesworth SE, MA Baber and IA Caplan. (1996). Cytokine expression by human marrow-derived mesenchymal progenitor cells in vitro: effects of dexamethasone and IL-1 alpha. J Cell Physiol 166:585–592.
42. Kinnaird T, E Stabile, MS Burnett and SE Epstein. (2004). Bone-marrow-derived cells for enhancing collateral development: mechanisms, animal data, and initial clinical experiences. Circ Res 95:354–363.
43. Leedham SJ, M Brittan, SA McDonald and NA Wright. (2005). Intestinal stem cells. J Cell Mol Med 9:11–24.
44. Togel F, Z Hu, K Weiss, J Isaac, C Lange and C Westenfelder. (2005). Administered mesenchymal stem cells protect against ischemic acute renal failure through differ-

entiation-independent mechanisms. Am J Physiol Renal Physiol 289:F31–F42.
45. Van Overstraeten-Schlogel N, Y Beguin and A Gothot. (2006). Role of stromal-derived factor-1 in the hematopoietic-supporting activity of human mesenchymal stem cells. Eur J Haematol 76:488–493.
46. Miyahara Y, N Nagaya, M Kataoka, B Yanagawa, K Tanaka, H Hao, K Ishino, H Ishida, T Shimizu, et al. (2006). Monolayered mesenchymal stem cells repair scarred myocardium after myocardial infarction. Nat Med 12:459–465.
47. Kinnaird T, E Stabile, MS Burnett, CW Lee, S Barr, S Fuchs and SE Epstein. (2004). Marrow-derived stromal cells express genes encoding a broad spectrum of arteriogenic cytokines and promote in vitro and in vivo arteriogenesis through paracrine mechanisms. Circ Res 94:678–685.
48. Shake JG, PJ Gruber, WA Baumgartner, G Senechal, J Meyers, JM Redmond, MF Pittenger and BJ Martin. (2002). Mesenchymal stem cell implantation in a swine myocardial infarct model: engraftment and functional effects. Ann Thorac Surg 73:1919–1925, discussion 1926.
49. Bir SC, J Esaki, A Marui, H Sakaguchi, CG Kevil, T Ikeda, M Komeda, Y Tabata and R Sakata. (2011). Therapeutic treatment with sustained-release platelet-rich plasma restores blood perfusion by augmenting ischemia-induced angiogenesis and arteriogenesis in diabetic mice. J Vasc Res 48:195–205.
50. Das H, JC George, M Joseph, M Das, N Abdulhameed, A Blitz, M Khan, R Sakthivel, HQ Mao, et al. (2009). Stem cell therapy with overexpressed VEGF and PDGF genes improves cardiac function in a rat infarct model. PLoS One 4:e7325.
51. Schlessinger J. (2000). Cell signaling by receptor tyrosine kinases. Cell 103:211–225.
52. Stratman AN, AE Schwindt, KM Malotte and GE Davis. (2010). Endothelial-derived PDGF-BB and HB-EGF coordinately regulate pericyte recruitment during vasculogenic tube assembly and stabilization. Blood 116:4720–4730.
53. Lindahl P, BR Johansson, P Leveen and C Betsholtz. (1997). Pericyte loss and microaneurysm formation in PDGF-B-deficient mice. Science 277:242–245.
54. Wang H, Y Yin, W Li, X Zhao, Y Yu, J Zhu, Z Qin, Q Wang, K Wang, et al. (2012). Over-expression of PDGFR-beta promotes PDGF-induced proliferation, migration, and angiogenesis of EPCs through PI3K/Akt signaling pathway. PLoS One 7:e30503.
55. Floege J, F Eitner and CE Alpers. (2008). A new look at platelet-derived growth factor in renal disease. J Am Soc Nephrol 19:12–23.
56. Casella I, T Feccia, C Chelucci, P Samoggia, G Castelli, R Guerriero, I Parolini, E Petrucci, E Pelosi, et al. (2003). Autocrine-paracrine VEGF loops potentiate the maturation of megakaryocytic precursors through Flt1 receptor. Blood 101:1316–1323.
57. Gerber HP, AK Malik, GP Solar, D Sherman, XH Liang, G Meng, K Hong, JC Marsters and N Ferrara. (2002). VEGF regulates haematopoietic stem cell survival by an internal autocrine loop mechanism. Nature 417:954–958.
58. Furumatsu T, ZN Shen, A Kawai, K Nishida, H Manabe, T Oohashi, H Inoue and Y Ninomiya. (2003). Vascular endothelial growth factor principally acts as the main angiogenic factor in the early stage of human osteoblastogenesis. J Biochem 133:633–639.
59. Ball SG, CA Shuttleworth and CM Kielty. (2007). Vascular endothelial growth factor can signal through platelet-derived growth factor receptors. J Cell Biol 177:489–500.
60. Senftleben U and M Karin. (2002). The IKK/NF-kappa B pathway. Criti Care Med 30:S18–S26.
61. Herrmann JL, BR Weil, AM Abarbanell, Y Wang, JA Poynter, MC Manukyan and DR Meldrum. (2011). IL-6 and TGF-alpha costimulate mesenchymal stem cell vascular endothelial growth factor production by ERK-, JNK-, and PI3K-mediated mechanisms. Shock 35:512–516.
62. Tallquist M and A Kazlauskas. (2004). PDGF signaling in cells and mice. Cytokine Growth Factor Rev 15:205–213.
63. Hung SC, RR Pochampally, SC Chen, SC Hsu and DJ Prockop. (2007). Angiogenic effects of human multipotent stromal cell conditioned medium activate the PI3K-Akt pathway in hypoxic endothelial cells to inhibit apoptosis, increase survival, and stimulate angiogenesis. Stem Cells 25:2363–2370.
64. Brunet A, A Bonni, MJ Zigmond, MZ Lin, P Juo, LS Hu, MJ Anderson, KC Arden, J Blenis and ME Greenberg. (1999). Akt promotes cell survival by phosphorylating and inhibiting a Forkhead transcription factor. Cell 96:857–868.
65. Franke TF, DR Kaplan and LC Cantley. (1997). PI3K: downstream AKTion blocks apoptosis. Cell 88:435–437.
66. Datta SR, A Brunet and ME Greenberg. (1999). Cellular survival: a play in three Akts. Genes Dev 13:2905–2927.
67. Bekhite MM, A Finkensieper, S Binas, J Muller, R Wetzker, HR Figulla, H Sauer and M Wartenberg. (2011). VEGF-mediated PI3K class IA and PKC signaling in cardiomyogenesis and vasculogenesis of mouse embryonic stem cells. J Cell Sci 124:1819–1830.
68. Ando H, K Nakanishi, M Shibata, K Hasegawa, K Yao and H Miyaji. (2006). Benidipine, a dihydropyridine-Ca2+ channel blocker, increases the endothelial differentiation of endothelial progenitor cells in vitro. Hypertens Res 29:1047–1054.
69. Chu L, H Hao, M Luo, Y Huang, Z Chen, T Lu, X Zhao, CM Verfaillie, JL Zweier and Z Liu. (2011). Ox-LDL modifies the behaviour of bone marrow stem cells and impairs their endothelial differentiation via inhibition of Akt phosphorylation. J Cell Mol Med 15:423–432.
70. Hoffmann A, A Levchenko, ML Scott and D Baltimore. (2002). The IkappaB-NF-kappaB signaling module: temporal control and selective gene activation. Science 298:1241–1245.
71. Kuhnel F, L Zender, Y Paul, MK Tietze, C Trautwein, M Manns and S Kubicka. (2000). NFkappaB mediates apoptosis through transcriptional activation of Fas (CD95) in adenoviral hepatitis. J Biol Chem 275:6421–6427.
72. Misra A, SB Haudek, P Knuefermann, JG Vallejo, ZJ Chen, LH Michael, N Sivasubramanian, EN Olson, ML Entman and LD Mann. (2003). Nuclear factor-kappaB protects the adult cardiac myocyte against ischemia-induced apoptosis in a murine model of acute myocardial infarction. Circulation 108:3075–3078.
73. Pahl HL. (1999). Activators and target genes of Rel/NF-kappaB transcription factors. Oncogene 18:6853–6866.
74. Karin M and A Lin. (2002). NF-kappaB at the crossroads of life and death. Nat Immunol 3:221–227.
75. Becker C, MC Fantini, C Schramm, HA Lehr, S Wirtz, A Nikolaev, J Burg, S Strand, R Kiesslich, et al. (2004). TGF-beta suppresses tumor progression in colon cancer by inhibition of IL-6 trans-signaling. Immunity 21:491–501.
76. Gross A, J Jockel, MC Wei and JS Korsmeyer. (1998). Enforced dimerization of BAX results in its translocation, mitochondrial dysfunction and apoptosis. EMBO J 17:3878–3885.
77. Yang E and SJ Korsmeyer. (1996). Molecular thanatopsis: a discourse on the BCL2 family and cell death. Blood 88: 386–401.

78. Ashkenazi A and VM Dixit. (1998). Death receptors: signaling and modulation. Science 281:1305–1308.
79. Nishikawa S, T Tatsumi, J Shiraishi, S Matsunaga, M Takeda, A Mano, M Kobara, N Keira, M Okigaki, et al. (2006). Nicorandil regulates Bcl-2 family proteins and protects cardiac myocytes against hypoxia-induced apoptosis. J Mol Cell Cardiol 40:510–519.

Address correspondence to:
Prof. Xiaobing Fu
Burns Institute
Trauma Center of Postgraduate Medical College
The First Affiliated Hospital
General Hospital of PLA
51 Fu Cheng Road
Beijing 100048
People's Republic of China

E-mail: fuxb@cgw.net.cn; fuxiaobing@vip.sina.com

Prof. Biao Cheng
The Key Laboratory of Trauma Treatment
& Tissue Repair of Tropical Area, PLA
Department of Plastic Surgery
Guangzhou General Hospital of Guangzhou Command
GuangDong
Guangzhou 510010
People's Republic of China

E-mail: chengbiaocheng@sohu.com.

Received for publication January 30, 2013
Accepted after revision July 25, 2013
Prepublished on Liebert Instant Online July 25, 2013